

Interplanetary Coronal Mass Ejection of October 3, 2021

J. J. Blanco,^{a,*} D. Arrazola^a and M. A. Hidalgo^a

^a*University of Alcalá,*

UAH Campus Científico Tecnológico (Externo) Ctra Madrid-Barcelona, 33,600. 28802 Alcalá de Henares (Madrid), Spain

E-mail: juanjo.blanco@uah.es

Magnetic clouds are closed structures immersed within interplanetary coronal mass ejections. These structures have an important effect on the propagation of solar energetic particles and cosmic rays that is observed as variations in the flux of these particle populations. On November 3, 2021 one of these structures was observed at different solar distances by instruments aboard Solar Orbiter and instruments in Earth orbit. The topology of the magnetic cloud has been analyzed by observing its evolution between the different observation points and the effect on solar energetic particles and cosmic rays

38th International Cosmic Ray Conference (ICRC2023)
26 July - 3 August, 2023
Nagoya, Japan



*Speaker

1. Introduction

Interplanetary Coronal Mass Ejections (ICMEs) are huge structures that emerge from the Sun very rapidly with velocities of up to 2000-3000 km/s. The transition from the corona to the interplanetary medium drags the ICMEs and their velocity can be reduced by as much as a factor of three to 1 AU. This process, together with the interaction of ICMEs with other interplanetary structures, such as interaction regions or other ICMEs, can modify the structure of the ICME.

The studies of the large structures known as ICMEs is more and more increasing because their interest by themselves and for impact in the Space Weather forecast and, hence, in the space technology development.

The in-situ observations of the ICMEs are associated with structured and ordered magnetic field topologies, and from the theoretical point of view the interest has been deposited in develop analytical or numerical models that allow to understand the physical mechanisms inside them, and not only in their origin but also during their evolution in the interplanetary medium and, hence, their interaction with other phenomena in it.

It is common to observe three clear regions in the ICME at 1 AU, the shock, the sheath and the magnetic cloud. The interactions discussed above can affect these three regions differently.

Therefore, since [1], who established the magnetic cloud (MC) definition from the magnetic field and solar wind plasma data, different models and techniques have appeared: from cylindrical approximation with circular cross section ([2]; [3]), including distortion on it ([4]; [5]), or local expansion ([6]). But the relaxation of such cylindrical approximation structures is necessary in order to connect the local with the global structure in a more realistic scene and, additionally, to understand its connection with the Sun, and its interactions with the solar wind during its movement in the interplanetary medium. Even more, with the possibility of multipoint spacecraft observations are now available, giving the opportunity to infer the structure of this large-scale magnetic flux ropes structures in the solar wind, providing information of its evolution. Attempts in this goal has been to assume spheroidal, plasmoid or toroidal structures ([7]; [8]; [9]). Furthermore, more recently, we have developed a series papers presenting a global model that allow to analytically approximate to this problem, ([10]), and which assumes torus topology for the MC. That is the model we have used for the analysis of November 2021 MC, using the data provide by ACE and SOLO spacecrafts. From the fitting of the model several physical parameters are obtained, although the most relevant for the present analysis correspond to the latitude, θ , respecting to the ecliptic plane, and the longitude, ϕ , respecting to the Sun-Earth line, of the axis of the MC.

Cosmic rays (CR) can also be used as a tool to analyze ICMEs. The structure of the ICME prevents cosmic rays from entering the ICME core and this is observed as a reduction of the CR flux during the passage of the ICME. These decreases are called Forbush decreases (FD) after the name of their discoverer [11]. Neutron monitors are used to study FDs, their relatively high statistics and their stability over very long periods of time make them the perfect instrument to study solar activity and in particular FDs.

Instruments that measure energetic particles aboard space missions are also valuable for studying FD. Although the energy range is usually ten times lower than that of the neutron monitor and direct comparison between the two is difficult, qualitative comparisons can be made. In addition, to study these events, counts are usually sufficient and it is not necessary to use the particle flux.

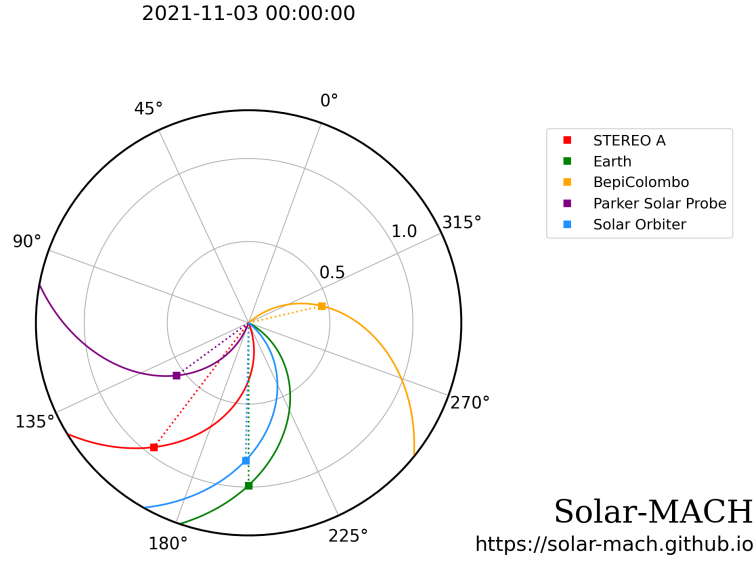


Figure 1: SoLO Earth relative position. Plot has been made with Solar-MACH tool [13]

This allows to increase the statistics of the measurements favoring the study of weaker structures or substructures [12].

In this work, the evolution of the MC observed at the beginning of November 2021 is analyzed using the observations by Solar Orbiter at 0.84 AU and Earth.

2. Solar and solar wind context

The Solar Orbiter spacecraft and Earth were radially aligned in early November 2021 (Figure 1). Both Solar Orbiter's in situ instruments and observatories on Earth observed an ICME. The Earth was at 0.99 AU and the Solar Orbiter was at 0.84. This vantage scenario allowed us to study radial effects during ICME propagation between the two observing points with smaller contributions from other ICME displacement-related effects.

Between late October 2021 and early November 2021, a series of consecutive X-flares were observed and reported by the GOES spacecraft. The October 28 X-flare at 15:35 UT was related to the origin of GLE73 [14] although it was not directly related to the ICME observed on Earth on November 3. The X flare, probably related to it, was the one that started on 2021/11/02 02:27UT reaching a peak flux at 03:07 UT (Figure 2). A halo CME erupted on 2021/11/02 02:48:05UT with a linear velocity of 1473 km/s (https://cdaw.gsfc.nasa.gov/CME_list/). Assuming radial propagation and constant velocity, the estimated arrival time of this ICME at Earth orbit was 2021/03/11 10:48UT.

The solar wind conditions on Earth are presented in Figure 4. The dashed vertical lines mark the shock, sheath, and magnetic cloud during the passage of the ICME past the Earth. The data are from the omniweb data explorer (<https://omniweb.gsfc.nasa.gov/form/dx1.html>). The arrival of the shock is clear and coincides with a sharp increase in magnetic field strength and solar wind speed. The sheath is characterized in this event by a highly fluctuating magnetic field and a relatively hot plasma. The nose of the MC marks the beginning of the smooth rotation of the

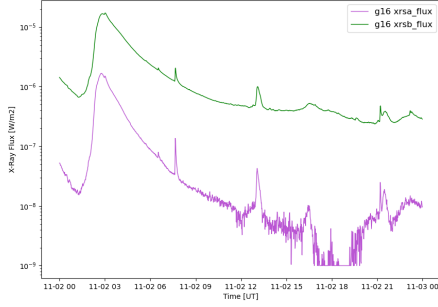


Figure 2: GOES X-ray measurements. Start time 02:27h. Flux peak at 03:07h

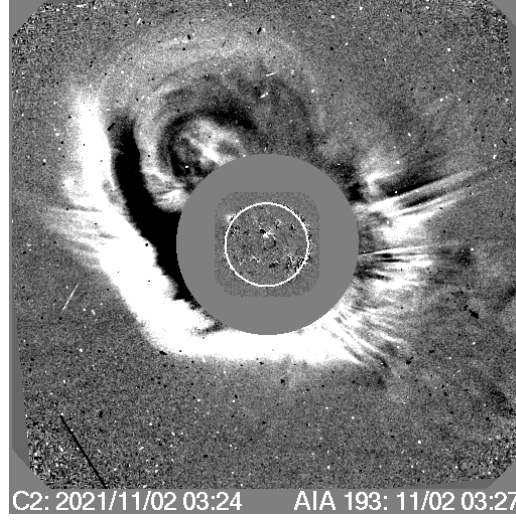


Figure 3: Halo 02-11-2021 02:48:05 ICME
https://cdaw.gsfc.nasa.gov/CME_list/

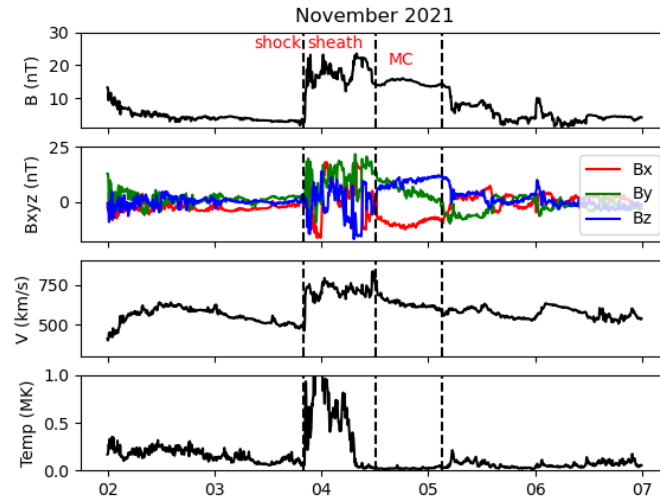


Figure 4: Solar wind at 1 AU. Magnetic field and its components in GSE, solar wind speed and temperature are presented.

magnetic field component and a smooth decrease in velocity along the MC. A relatively cold plasma is also observed along the MC passage.

3. The analytical model for the magnetic field

Here, we only summarize the expressions of the model for the magnetic field components used in our fittings, a detailed description of the model can be found in the series of works mentioned above, ([15],[16],[17], [18]). The model assumes for the MC a torus structure with a maximum variable radius cross-section along it, that we consider a circular cross-section. Choosing an appropriate

coordinate system to describe such a geometry we can obtained the theoretical expression for the magnetic field,

$$\vec{B} = B_\varphi \vec{e}_\varphi + B_\psi \vec{e}_\psi + B_\eta \vec{e}_\eta \quad (1)$$

where

$$B_\varphi = B_\varphi^0(\psi) \cos(\varphi) - \mu_0 j_\psi r \cosh(-\rho_0 \eta + f(\psi)) \quad (2)$$

is the poloidal component of the magnetic field, being μ_0 the vacuum permeability, ρ_0 the mean radius of the torus; r the radial parameter related to its elliptical cross-section (playing the role of the radius in the circular cross-section); φ the polar angle of the cross-section; ψ the angular coordinate of the axis of the torus, the axial angle; and η is the coordinate associated with the eccentricity of its cross-section, i.e., the distortion of the cloud, (that we will always suppose to be constant, i.e., $\eta = \text{cte}$, along the torus). $f(\psi)$ is the auxiliary function, depending on the coordinate ψ , and responsible of the angular dependence of the maximum radius of the cross-section of the MC along the torus, (if this function is constant the torus has a uniform cross-section along it). And j_ψ is the axial component of the total plasma current density. Finally, $B_\varphi^0(\psi)$ represents an integration constant that, if we consider magnetic flux conservation along the torus, we can express as

$$B_\varphi^0(\psi) = B_{0\varphi}^0 \sin\left(\frac{\psi}{2}\right) \quad (3)$$

where $B_{0\varphi}^0$ depends on r . On the other hand, the axial component of the magnetic field, given by

$$B_\psi = B_\psi^0(\psi) + \mu_0 j_\varphi r \cosh(-\rho_0 \eta + f(\psi)) \quad (4)$$

where $B_\psi^0(\psi)$ is the axial magnetic field at the axis of the torus, given by

$$B_\psi^0(\psi) = B_{0\psi}^0 \left| \cos\left(\frac{\psi}{2}\right) \right| \quad (5)$$

$B_{0\psi}^0$ imposing to be constant, and j_φ corresponds to the poloidal component of the plasma current density. To be able to use the analytical expressions of the components of the magnetic field we have to do some hypothesis about the behaviour of the different physical magnitudes appearing in them. The defined auxiliary function $f(\psi)$ allows us to assume and represent different MC topologies. Then, our hypothesis will be

$$f(\psi) = C \sin\left(\frac{\psi}{2}\right) \quad (6)$$

C being an adjustable constant.

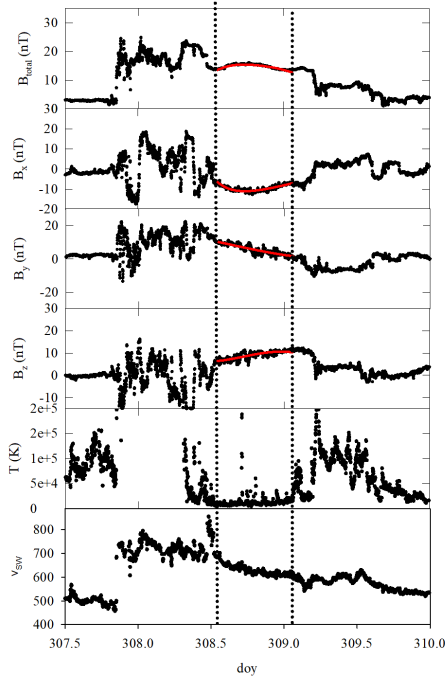
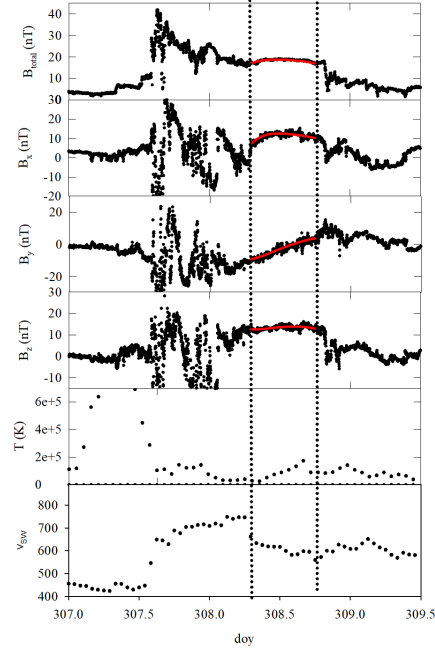
Eventually, the last component of the magnetic field has the expression

$$B_\eta = -2 \cos(\varphi) S \left\{ B_{0\psi}^0 \sin\left(\frac{\psi}{2}\right) \right\} + \frac{1}{C} \mu_0 \alpha (t_0 - t) r^2 \cosh(-\rho_0 \eta + f(\psi)) \quad (7)$$

where the term $S = \frac{\sqrt{\sin^2(\psi)}}{\sin(\psi)}$ corresponds to the Heaviside function.

Table 1: Latitude (θ) and longitude (ϕ) of the axis of the MC such as deduced from the fitting of the model to the data corresponding to each spacecraft.

	Spacecraft	SoLO (0.84 AU)	ACE (0.99 AU)
Fit parameter	θ	14°	1°
Fit parameter	ϕ	148°	176°

**Figure 5:** Data obtained by ACE for the magnetic cloud of November 2021, and the corresponding fits with the toroidal model.**Figure 6:** Data obtained by SOLO for the magnetic cloud of November 2021, and the corresponding fits with the toroidal mode (in red). The data represented is the same as in Figure 5

4. Data analysis

The aim of this work is to study the evolution of the MC when it is coming far from Sun. Figures 5 and 6 show from the top to the bottom the magnetic field strength, B , the Cartesian GSE-components (B_x , B_y , B_z) for ACE and RTN-components (B_x , B_y , B_z) for SOLO, the proton temperature and the bulk solar wind velocity. The vertical dot lines represent the time boundaries of the cloud. Superimposed on the experimental data the toroidal model predictions are represented with solid lines (in red).

Looking at the figures corresponding to the fittings with the model, and comparing the results obtained for the orientation of the magnetic cloud, and having in mind the location of both spacecrafts, we can ascertain that are observing the same structure. It is also clear the magnetic cloud is expanding, and according to the model's results, see Table 1, the MC axis is falling to the ecliptic plane and is aligning to the Sun-Earth line.

5. Conclusions

This is a work under development. Its aim is to study how the MC magnetic topology can change in its way running away from solar gravity well. The magnetic topology has been analyzed with the toroidal model by ([15],[16],[17],[18]). The initial conclusion is that the MC orientation is changing with respect the Sun-Earth line being more aligned with this line and the MC axis slope with respect the ecliptic plane is decreasing at 1AU.

As a preliminary work some steps must to be done before consider this analysis as definitive. One is to include in the analysis the solar energetic particle and cosmic ray flux and the other one a deeper study of the 3-D structure of the MC at SOLO and Earth position.

Acknowledgments

Thanks to the project PID2019-107806GB-I00, funded by Ministerio de Ciencia e Innovación

References

- [1] L. Burlaga, E. Sittler, F. Mariani and R. Schwenn, *Magnetic loop behind an interplanetary shock: Voyager, helios, and imp 8 observations*, *Journal of Geophysical Research: Space Physics* **86** (1981) 6673 [<https://agupubs.onlinelibrary.wiley.com/doi/pdf/10.1029/JA086iA08p06673>].
- [2] R. Lepping, J. Jones and L. Burlaga, *Magnetic field structure of interplanetary magnetic clouds at 1 au*, *Journal of Geophysical Research: Space Physics* **95** (1990) 11957.
- [3] M. Hidalgo, C. Cid, A. Vinas and J. Sequeiros, *A non-force-free approach to the topology of magnetic clouds in the solar wind*, *Journal of Geophysical Research: Space Physics* **107** (2002) SSH1.
- [4] T. Mulligan and C. Russell, *Multispacecraft modeling of the flux rope structure of interplanetary coronal mass ejections: Cylindrically symmetric versus nonsymmetric topologies*, *Journal of Geophysical Research: Space Physics* **106** (2001) 10581.
- [5] M. Hidalgo, T. Nieves-Chinchilla and C. Cid, *Elliptical cross-section model for the magnetic topology of magnetic clouds*, *Geophysical research letters* **29** (2002) 15.
- [6] C.J. Farrugia, V. Osherovich and L. Burlaga, *Magnetic flux rope versus the spheromak as models for interplanetary magnetic clouds*, *Journal of Geophysical Research: Space Physics* **100** (1995) 12293.
- [7] K. Ivanov, A. Harshiladze, E. Eroshenko and V. Styazhkin, *Configuration, structure, and dynamics of magnetic clouds from solar flares in light of measurements on board vega 1 and vega 2 in january–february 1986*, *Solar physics* **120** (1989) 407.
- [8] M. Vandas, S. Fischer, P. Pelant and A. Geranios, *Spheroidal models of magnetic clouds and their comparison with spacecraft measurements*, *Journal of Geophysical Research: Space Physics* **98** (1993) 11467.

- [9] E. Romashets and M. Vandas, *Dynamics of a toroidal magnetic cloud in the solar wind*, *Journal of Geophysical Research: Space Physics* **106** (2001) 10615.
- [10] M. Hidalgo and T. Nieves-Chinchilla, *A global magnetic topology model for magnetic clouds. i.*, *The Astrophysical Journal* **748** (2012) 109.
- [11] S.E. Forbush, *On the effects in cosmic-ray intensity observed during the recent magnetic storm*, *Phys. Rev.* **51** (1937) 1108.
- [12] Blanco, J. J., Hidalgo, M. A., Gómez-Herrero, R., Rodríguez-Pacheco, J., Heber, B., Wimmer-Schweingruber, R. F. et al., *Energetic-particle-flux decreases related to magnetic cloud passages as observed by the helios 1 and 2 spacecraft*, *A&A* **556** (2013) A146.
- [13] J. Gieseler, N. Dresing, C. Palmroos, J.L. Freiherr von Forstner, D.J. Price, R. Vainio et al., *Solar-mach: An open-source tool to analyze solar magnetic connection configurations*, *Frontiers in Astronomy and Space Sciences* **9** (2023) .
- [14] Papaioannou, A., Kouloumvakos, A., Mishev, A., Vainio, R., Usoskin, I., Herbst, K. et al., *The first ground-level enhancement of solar cycle 25 on 28 october 2021*, *A&A* **660** (2022) L5.
- [15] M.A. Hidalgo and T. Nieves-Chinchilla, *A global magnetic topology model for magnetic clouds. i.*, *The Astrophysical Journal* **748** (2012) 109.
- [16] M. Hidalgo, *A global magnetic topology model for magnetic clouds. ii.*, *The Astrophysical Journal* **766** (2013) 125.
- [17] M. Hidalgo, *A global magnetic topology model for magnetic clouds. iii.*, *The Astrophysical Journal* **784** (2014) 67.
- [18] M. Hidalgo, *A global magnetic topology model for magnetic clouds. iv.*, *The Astrophysical Journal* **823** (2016) 3.